Ore Geology Reviews 73 (2016) 284–297

Contents lists available at ScienceDirect

Ore Geology Reviews

journal homepage: www.elsevier.com/locate/oregeorev

The age, geological setting, and types of gold deposits in the Yanbian and adjacent areas, NE China

Yun-Sheng Ren [a,*], Cong Chen [a], Xin-Tong Zou [a], Hua-Lei Zhao [b], Yu-Jie Hao [a], He-Nan Hou [a], Zhao-Chu Hu [c], Guo-Hao Jiang [d]

[a] College of Earth Sciences, Jilin University, Changchun 130061, China
[b] Tianjin Institute of Geology and Mineral Resources, Tianjin 300170, China
[c] State Key Laboratory of Geological Processes and Mineral Resources, China University of Geosciences, Wuhan 430074, China
[d] State Key Laboratory of Ore Deposit Geochemistry, Institute of Geochemistry, Chinese Academy of Sciences, Guiyang 550002, China

ARTICLE INFO

Article history:
Received 28 April 2014
Received in revised form 16 March 2015
Accepted 18 March 2015
Available online 19 March 2015

Keywords:
Gold deposit types
Orogenic
Tectonics
Zircon U–Pb dating
Yanbian, NE China

ABSTRACT

The eastern part of the Xing'an–Mongolian Orogenic Belt (XMOB) in Jilin and Heilongjiang Provinces, NE China, is highly prospective for gold mineralization, and more than ten gold and gold–copper deposits have been found in the Yanbian and Dongning areas in the last decade. These deposits are classified, based on geological characteristics and mineralogical and geochemical information, into orogenic, intrusion-related, gold-rich porphyry, and epithermal deposits; the latter are further divided into high-sulfidation (HS) and low-sulfidation (LS) deposit types.

We present the results of zircon laser ablation U–Pb dating of some representative gold deposits and associated magmatic rocks within the eastern XMOB; these are the orogenic Wudaogou deposit, the intrusion-related Naozhi deposit, and the epithermal Jiusangou gold deposit. The weighted mean age of the granodiorite that hosts mineralization at Wudaogou is 253.1 ± 0.3 Ma, whereas zircons from a porphyritic dacite dike that was intruded at the same time as the formation of the Naozhi deposit yielded two groups of weighted mean ages (198.9 ± 3.6 and 126.3 ± 1.7 Ma). Zircons from a porphyritic quartz diorite within the breccia that hosts the Jiusangou deposit yielded a weighted mean age of 108.1 ± 1.4 Ma.

These data, combined with data from previous studies, enable the identification of three periods of Phanerozoic gold mineralization within the Yanbian area and adjacent regions; these are ca. 270–240, ca. 130–120, and ca. 115–100 Ma. The Late Permian to Early Triassic (270–240 Ma) events formed the orogenic gold deposits at Yangjingou and Wudaogou; both are located near the Xar Moron–Changchun Suture Zone between the North China Craton and the XMOB. The Early Cretaceous (130–120 Ma) events produced intrusion-related gold mineralization, such as the Naozhi and Miantian deposits, which are associated with Jurassic granodiorite plutons or volcanic rocks. Almost all of the gold-rich porphyry and epithermal gold deposits in this area formed during the late Early Cretaceous (115–110 Ma). We propose that the orogenic gold mineralization in the Yanbian area was closely related to the collision between the North China Craton and the eastern XMOB, whereas the other gold deposit types formed at Early Cretaceous lithospheric extensions associated with post-subduction tectonics.

1. Introduction

The Yanbian area in NE China and surrounding regions are located within the eastern Xing'an–Mongolian Orogenic Belt (XMOB), in the eastern segment of the Central Asian Orogenic Belt (CAOB). The area is bounded by the Xar Moron–Changchun Suture Zone to the south and by the Dunhua–Mishan fault to the northwest. A recently proposed nomenclature for tectonic units in this area (Jia et al., 2004; Wu et al., 2007, 2011; Lin et al., 2008) suggests that this region is bounded by the North China Craton and by the Songliao, Khanka, Jiamusi, and Nadanhada terranes (Fig. 1a). The area underwent intensive and widespread tectonism and magmatism when it was part of the Paleo-Asian Ocean and Paleo-Pacific tectonic domains, leading to the development of numerous Phanerozoic intrusions that crop out over an area of ~20,000 km^2 (Zhang, 2002). This magmatism is also associated with significant gold, copper, lead and zinc, molybdenum, tungsten, and iron mineralization. Recent research work in this area has focused on characterizing the tectonic evolution, the amalgamation of microcontinental blocks, regional magmatic events, and ore genesis (Meng et al., 2001; Zhao, 2007; Men, 2011; Wu et al., 2007, 2011; Zhao et al., 2013).

The Yanbian area is one of the most important areas of gold mineralization in NE China. To date, two large-sized deposits (a total of ≥20 t contained gold reserves; the Xiaoxi'nancha and Jinchang

* Corresponding author.
E-mail address: renys@jlu.edu.cn (Y.-S. Ren).

http://dx.doi.org/10.1016/j.oregeorev.2015.03.013
0169-1368/

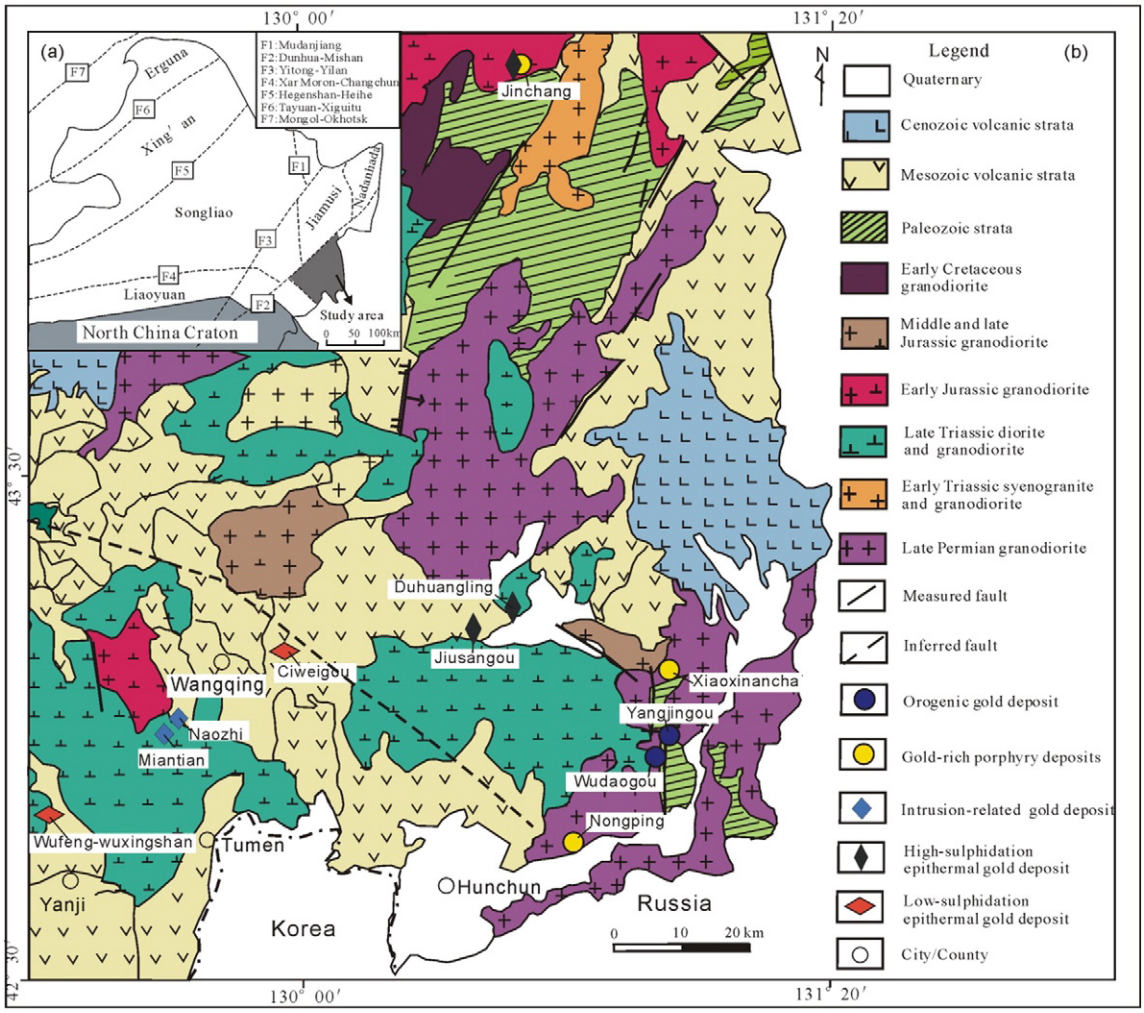

Fig. 1. Tectonic position map (a, modified from Wu et al. (2011)), regional geology and distribution map of gold deposits in Yanbian and adjacent areas (b, modified from Men, 2011).

deposits), four medium-sized deposits (a total of ≥5 t contained gold reserves < 20 t; the Wufeng–Wuxingshan, Naozhi, Ciweigou, and Nongping deposits), and five small gold deposits (a total of <5 t contained gold reserves; the Yangjingou, Wudaogou, Miantian, Duhuangling, and Jiusangou deposits) have been discovered (Fig. 1b and Table 1). These deposits have been examined in terms of metallogenesis, ore deposit geology, the composition of ore-forming fluid, geochronology, and ore genesis (Rui et al., 1995; Feng, 1998; Jia et al., 2001, 2011; Meng et al., 2001; Chai et al., 2002; Zhao, 2007; Sun et al., 2008a, 2008b; Men, 2011; Men et al., 2011; Ren et al., 2011, 2012). However, there is a lack of data on the genetic classification of the gold deposits, the age of metallogenesis, the tectonic setting of some of the more important deposits, and the nature of regional gold metallogenic systems.

This paper reviews all the available data for the above deposits and their tectonic setting, and provides a framework for the metallogenesis, geology, and tectonic evolution of the Yanbian area and adjacent regions. Zircon U–Pb isotopic dating of intrusions which is closely associated with gold mineralization in some representative deposits allows a synthesis and re-interpretation of existing geochronological data for the belt.

2. Regional geological setting

The pre-Middle to Late Triassic XMOB was bordered by the Siberian craton to the north, the Sino-Korean craton to the south, and the Pacific Ocean to the east, and comprised (from west to east) the Erguna, Xing'an, Songliao, Jiamusi, Khanka, and Nadanhada terranes. The Phanerozoic geological evolution of NE China is divided into two periods (Wu et al., 2011): an early period associated with the Paleozoic closure of the Paleo-Asian Ocean and a later period associated with Mesozoic subduction of the Paleo-Pacific Plate.

The metamorphic rocks in the study area are the Huangsong, Qinglongcun, and Wudaogou groups, which contain low- to medium-grade metamorphosed volcanic and sedimentary rocks that include metamorphosed porphyritic andesite, carbonaceous sericite phyllite, quartz schist, granulite, biotite schist, marble, amphibole schist, and sandy slate units. The Huangsong Group crops out in the Dongning area and farther to the NE of this area, whereas the Qinglongcun Group crops out along the NW–SE trending regional Gudonghe fault zone in the southern Yanbian area. The Wudaogou Group is sparsely exposed in a N–S belt within the Hunchun and Wangqing areas (Fig. 1b).

The lower Permian rock units in the study area include molasse units of the Kaishantun Formation and pyroclastic units of the Miaoling Formation. The upper Permian units comprise intercalated marine and terrestrial clastic sediments of the Jiefangcun Formation and pyroclastic rocks and turbidites of the Kedao Formation, all of which indicate a change in sedimentary environment from marine to terrigenous sediments or to intercalated marine and terrigenous sediments. The Mesozoic rocks in this area are continental volcanic and volcano-sedimentary rocks that are dominated by Late Jurassic medium- and high-K calc-alkalic andesitic rocks, with lesser Cretaceous calc-alkaline basaltic andesite units.

The Mesozoic history of NE China is dominated by the influence of the subduction of the Paleo-Pacific Plate, a tectonic event that caused

Table 1
Types and geological characteristics of gold deposits in Yanbian and adjacent areas. Summarized from Qi et al. (2005), Jia et al. (2011), Men (2011), Hou et al. (2012), Han et al. (2013), Zhao et al. (2013), Zhang et al. (2014) and this paper.

Deposit type	Examples	Ore-hosting rocks	Orebody	Gold reserves/tonnes	Metal minerals	Alteration types	Other key features
Orogenic	Yangjingou	Late Permian monzogranite; low-grade metamorphic rocks of the Wudaogou Group	Quartz vein and altered-rock controlled by faults	<5	Major: pyrite, arsenopyrite; minor: molybdenite, chalcopyrite and native gold	Silicification, sericitization, phyllic alteration, chloritization, carbonation	≤5% sulfides; ore-forming temperature 230–270 °C; depth 2.35 km
	Wudaogou	Late Permian altered granite	Quartz vein and altered granodiorite controlled by NW-extending faults	<5	Major: pyrite, arsenopyrite; minor: chalcopyrite, pyrrhotite and native gold and electrum	Silicification, sericitization, greisenization, phyllic alteration, carbonation	Near to Yangjingou and both located south to the Xar Moron–Changchun Suture Zone
Intrusion-related	Naozhi	Early Jurassic granite; Cretaceous andesitic volcanic rock and porphyritic dacite dykes	Sulfide–quartz veins, veinlet and disseminated	4.5	Major: pyrite, chalcopyrite, galena and sphalerite; minor: tetrahedrite, bornite, chalcocite and gold minerals	Sericitization, silicification, propylitization and K-feldspar	Ore-forming temperature 200–320 °C; ore fluid composed mainly of magmatic water and minor surface water
	Miantian	Early Jurassic granodiorite	Sulfide–quartz veins	1.99	Major: pyrite, chalcopyrite, galena and sphalerite; minor: chalcocite, bornite, magnetite and gold minerals	Phyllic alteration, silicification, propylitization, argillization, carbonation and K-feldspar	Ore-forming temperature 200–340 °C; ore fluid: major from magmatic water and minor from surface water
Gold-rich porphyry	Xiaoxinancha	Late Permian granite, diorite and porphyritic granite; low-grade metamorphic rocks of the Wudaogou Group	Sulfide veinlet, sulfide-bearing quartz vein; veinlet and disseminated altered rock	96	Major: chalcopyrite, pyrite and pyrrhotite; minor: molybdenite, melnikovite, bornite, galena, sphalerite, native gold and electrum	Sericitization, silicification, propylitization, argillization, carbonation minor: K-feldspar and biotitization	Ore-forming temperature 220–360 °C; high salinity; boiling fluid major from magmatic water mixed by surface water
	Nongping	Early Cretaceous granodiorite and associated porphyritic diorite veins	Veins, veinlets and disseminated	3	Major: pyrite, pyrrhotite and chalcopyrite; minor: sphalerite, galena, gold minerals	Biotitization, sericitization, silicification, propylitization, argillization, chloritization	Linear and planar alteration zonation; boiling ore fluid
	No. 18 orebody in Jinchang	Early Cretaceous extensively altered granitoid and porphyritic granite	Disseminated sulfides and fine quartz–sulfide stockworks or veinlets	70	Pyrite and chalcopyrite (>5%); minor: sphalerite, galena, native gold, and electrum	Phyllic alteration; minor: silicification, argillization, K-feldspar and biotitization	Ore-forming temperatures from 480 °C to 200 °C, from high to low salinities; boiling ore-forming fluid associated with oxidized intrusion
HS epithermal	Jiusangou	Early Cretaceous porphyritic quartz diorite and andesitic pyroclastic rock	Brecciated, veinlet and disseminated, crypto-explosive breccia pipes	1.5	Major: pyrite (<10%); minor: arsenopyrite, chalcopyrite, tetrahedrite, chalcocite, electrum and native gold	Sericitization, silicification, propylitic alteration, kaolinization and carbonation	Ore fluid: 300 °C–200 °C, variable salinities, high oxidation, magmatic water mixed by meteoric water
	Duhuangling	Early Cretaceous quartz diorite, granitoid complexes and porphyritic granite veins	Veinlet and disseminated, sulfide–quartz vein and crypto-explosive breccia pipes	3.1	Major: pyrite (<15%); minor: chalcopyrite, bornite, pyrrhotite, arsenopyrite, galena, and less electrum, native gold and silver mineral	Phyllic alteration, silicification, carbonation, chloritization, argillic alteration and propylitic alteration	Depth: 0.7–1.4 km; temperature: 340 °C–280 °C
	No. J-1 orebody in Jinchang	Jurassic granitoid complexes and associated porphyritic diorite veins	Crypto-explosive breccias	–	Major: pyrite (<5%); minor: chalcopyrite, galena, native gold and electrum	Sericitization, silicification, kaolinization, chloritization and carbonation	Boiling ore-forming fluid; depth: <2.0 km
LS epithermal	Ciweigou	Jurassic andesitic volcanic clastic rock and lava rock	Auriferous quartz–calcite vein	<1	<5%, pyrite, chalcopyrite, tetrahedrite, sphalerite, electrum and argentite	Sericitization, silicification, adularization, kaolinization, carbonation and propylitic alteration	Temperature: 240 °C–200 °C; depth: 0.27–1.26 km; ore fluid major from surface water
	Wufeng–Wuxingshan	Wufeng: Early Cretaceous andesitic pyroclastic rock and lava rock; Wuxingshan: alkali feldspar granite, granite aplite and subvolcanics	Sulfide–quartz–calcite vein; Wuxingshan: veinlet, disseminated and quartz vein	5–20	<5%, pyrite, chalcopyrite, tetrahedrite, sphalerite, galena, electrum, argentite, calaverite, hessite and argentite	Silicification, adularization, kaolinization, sericitization, chloritization and zeolitization	Temperature: 280 °C–150 °C; depth: 0.15–0.65 km; ore fluid major from surface water

large-scale magmatism and mineralization. This area has recorded these magmatic metallogenic events, thereby considered as one of the more geologically important regions within the eastern Asian continental margin. Isotopic ages for plutons in this area, as reported by Zhang (2002), Sun et al. (2008a, 2008b), Fu (2009), Fu et al. (2010), Men (2011), and Wu et al. (2011), indicate that Phanerozoic magmatism in the Yanbian region can be divided into six periods: late Permian to Early Triassic (270–245 Ma), Late Triassic (225–220 Ma), Early Jurassic (200–180 Ma), Middle–Late Jurassic (170–150 Ma), early period of Early Cretaceous (135–120 Ma), and late period of Early Cretaceous (115–105 Ma).

Four groups of faults have been identified in the study area. The earliest E–W faults control the distribution of some early Paleozoic strata, and NW–SW faults are parallel to the Xar Moron–Changchun Suture Zone and were remobilized during the late Mesozoic. The well-developed NE–SW and NNE–SSW faults were active between the Late Triassic and the Cenozoic, and N–S trending faults occur within the central and eastern parts of the study area. The gold deposits in this area are generally associated with the E–W, NE–SW and NW–SW trending faults, and individual orebodies are controlled mainly by NW–SW, NNW–SSW or NE–SW trending fractures.

3. Types and characteristics of the gold deposits

The genetic classification of gold deposits in the study area remains controversial. For example, the genetic relationship between gold mineralization and porphyry deposits in the Mesozoic volcanic and intrusive rocks led Meng et al. (2001) to classify gold and gold–copper deposits in the Yanbian area as "porphyry and hydrothermal lode" deposits. However, Zhao (2007) and Men (2011) classified gold deposits in the Yanbian–Dongning area into porphyry deposits (e.g., the No. 18 orebody within the Jinchang and Nongping deposits), porphyry-like deposits (e.g., the Xiaoxi'nancha deposit), high-sulfidation (HS) epithermal deposits (e.g., the Naozhi, Jiusangou, Duhuangling deposits, and the No. J-1 orebody within the Jinchang deposit), and low-sulfidation (LS) epithermal type deposits (e.g., the Ciweigou and Wufeng–Wuxingshan deposits). Jia et al. (2011) also suggested that mesothermal lode gold deposits (e.g., the Naozhi and Duhuangling deposits) were present in this area in addition to the HS and LS epithermal gold deposits, and classified the Xiaoxi'nancha and Yangjingou gold deposits as hypothermal lode type gold deposits. Other researchers have also identified orogenic gold deposits in the Yanbian area, as exemplified by the Yangjingou deposit (Zhao et al., 2013).

Here, we investigate the ore-forming conditions, geological and geochemical characteristics, ore fluid compositions, and the spatial and temporal distribution of mineralization in this area, and on this basis divide the gold deposits into orogenic, intrusion-related, gold-rich porphyry, and epithermal types of deposits, with epithermal deposits being further divided into high-sulfidation (HS) and low-sulfidation (LS) subtypes. The gold deposit types and sub-types, and their characteristics, are listed in Table 1. Representative examples of the deposits are discussed below.

3.1. The Wudaogou orogenic gold deposit

Zhao et al. (2013) discussed the geology, timing of formation, and tectonic setting of the Yangjingou orogenic gold deposit, the first to be discovered in the Yanbian area. This area also hosts the recently discovered Wudaogou gold deposit, located 1 km south of the Yangjingou deposit and which may also be an orogenic gold deposit (Fig. 1b).

The Wudaogou gold deposit has characteristics similar to those of the Yangjingou deposit and consists of six gold orebodies within an altered granodiorite that are controlled by NW–SE and NNW–SSW trending compressional shear-related faults (Table 1 and Fig. 2). These orebodies comprise gold-bearing altered country rock and sulfide–quartz vein types of mineralization. The orebodies generally dip to the southwest at 25°–50°, have thick tabular or lenticular shapes, and have lengths of 50 to 400 m, widths of 0.5 to 3.0 m, and their gold grades are from 3–6 ppm.

Gold within the deposit is hosted by sulfide–quartz veins and altered country rock, and is associated with pyrite, arsenopyrite, molybdenite, and chalcopyrite in a gangue of quartz, muscovite, chlorite, sericite, and calcite. Sulfides within the deposit commonly have automorphic–subhedral granular and metasomatic relict textures and are generally either disseminated or are hosted by thin banded veins. The mineralization within the deposit is associated with silicification, and sericite and phyllic alteration, as well as the presence of other hydrothermal minerals such as muscovite, chlorite, and carbonate. Of these, only silicification and phyllic alteration are closely related to the gold mineralization.

The quartz within auriferous quartz veins in the deposit hosts two types of primary fluid inclusions: aqueous inclusions and CO_2-bearing three-phase inclusions. Petrographic and microthermometric analysis of these inclusions indicates that the deposit formed from NaCl–H_2O–CO_2 fluids with salinities of 3.37–15.65 wt.% NaCl equivalent and densities of 0.78–0.91 g/cm^3, with mineralization occurring at temperatures of 230 °C–270 °C. The deposit formed at estimated pressures of 15.85 to 30.22 MPa, with a mean pressure of 23.51 MPa that yields a depth of 2.35 km.

The ore-forming conditions, the characteristics of mineralization, and the ore-forming fluids associated with the Wudaogou gold deposit are similar to those of the Yangjingou deposit and other typical orogenic gold deposits in China and elsewhere (Groves et al., 2000; Goldfarb et al., 2001). This finding, combined with the depth of formation of this deposit (Groves et al., 1998), indicates that the Wudaogou deposit is an epizonal orogenic gold deposit.

3.2. The Naozhi intrusion-related gold deposit

Intrusion-related gold deposits in the study area are generally located in the region around Wangqing (Fig. 1b). The deposits of this type are hosted by Early Jurassic granodiorites or Late Jurassic–Early Cretaceous sub-volcanic rocks and are presumably controlled by faults or fractures. The gold mineralization within these deposits is associated with pyrite, chalcopyrite, sphalerite, galena, chalcocite, tetrahedrite, bornite, native gold, and electrum. The deposits are also associated with zoned alteration, from proximal phyllic alteration through zones of silicification and propylitic alteration to a distal zone of K-feldspar alteration that gives way to unaltered rock. These deposits formed at temperatures of 200 °C to 350 °C and at depths of 0.8 to >2.0 km.

The Naozhi deposit is located in the Mesozoic Wangqing volcanic basin (Fig. 1b). This area contains Quaternary sediments in addition to Middle Jurassic andesitic–dacitic–rhyolitic medium-K calc-alkaline volcanics (J_2t) and Late Jurassic andesitic–basaltic calc-alkaline volcanic rocks (J_3j). The faults in this area predominantly extend in NW, NE and EW directions and are usually intruded by dikes and filled by quartz veins. NW–SE trending fractures generally control the exposure of rock units as well as the location of mineralization in this area. Minor NE–SW and E–W trending faults are also developed. Voluminous Early Jurassic granodiorite intrusions and Early Cretaceous porphyritic dacite dike swarms are radially distributed along fractures and are closely spatially related to the gold mineralization (Fig. 3).

More than 20 mineralized alteration zones have been identified within the Naozhi deposit. The majority of these gold-bearing alteration zones are hosted by a granodiorite intrusion, although a few are hosted by volcanic rocks or porphyritic dacite dikes. The mineralization within the deposit is associated with silicification and with phyllic, kaolin, sericite, chlorite, and carbonate alteration, of which the silicification and the sericite and chlorite alteration are most closely linked with the mineralization. The largest alteration zone extends to the NW of the deposit, and it locally splits, re-joins, and pinches out. The majority of the orebodies within the deposit are auriferous quartz–sulfide veins

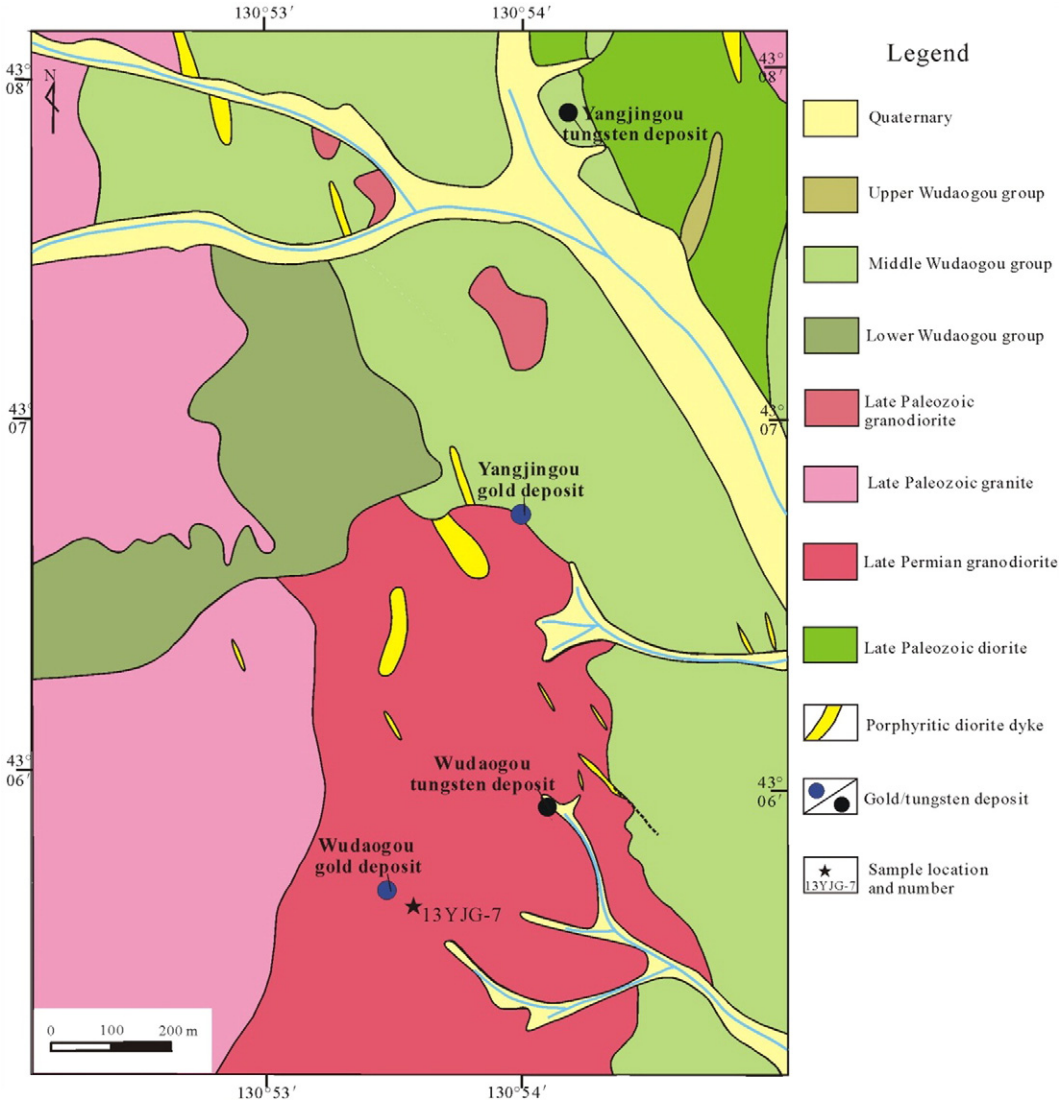

Fig. 2. Geology and deposit distribution map of Wudaogou–Yangjingou in eastern Hunchun area.

that have gentle wavy forms in both plan view and cross-section. These veins dip to the SW at 40°–60° and are ~600 m long.

The Naozhi deposit also hosts metal sulfides including pyrite and chalcopyrite, along with lesser amounts of galena, sphalerite, and minor chalcocite. The gold minerals in this deposit include native gold, electrum, and kustelite, all of which are present as inclusions, fracture-fills, and interstitial gold within pyrite and chalcopyrite. This mineralization is associated with a quartz, calcite, plagioclase, and sericite gangue that also contains minor amounts of chlorite, epidote, biotite, and K-feldspar.

Microthermometric analysis of fluid inclusions from the Naozhi deposit and the adjacent Miantian deposit indicates that the majority of mineralization formed at temperatures of 200 °C–320 °C and depths of 0.8–1.5 km (Wu, 2013). These fluid inclusions contain H_2O and CO_2 gas and represent the magmatic water that were derived from depth, mixed with minor amounts of meteoric water, and underwent minor boiling during ascent. The fluid inclusions have δD values of −94‰ and $\delta^{18}O_{water}$ values of −4.7‰, and plot between magmatic and meteoric fluid fields in a δD–$\delta^{18}O_{water}$ diagram, albeit closer to the magmatic water field, indicating that the fluids that formed these deposits were dominantly magmatic but underwent late-stage mixing with minor amounts of meteoric water (Huang, 1997; Meng et al., 2001).

The porphyritic dacite associated with the Naozhi deposit has initial $^{87}Sr/^{86}Sr$ values of 0.70342–0.7036, similar to rocks derived from the upper mantle ($^{87}Sr/^{86}Sr = 0.702–0.706$), indicating that this dacite formed from mantle-derived magmas (Huang, 1997; Cheng et al., 2009). Sulfides within the deposit have low $\delta^{34}S$ values with a small mean square error and range, indicating that they contain sulfur derived from the upper mantle or the lower crust (Huang, 1997; Su et al., 2003). These data indicate that all of the metals and fluids that formed the Naozhi gold deposit and associated alteration were sourced from depth.

The epizonal formation depth (0.8–1.5 km), combined with the fact that the deposit is hosted by a granodiorite, is closely related to subvolcanic rocks, has carbonic hydrothermal fluid characteristics, and contains stockwork and disseminated mineralization, both strongly suggest that the Naozhi deposit is an intrusion-related deposit (Sillitoe, 1991; Thompson et al., 1999; Goldfarb et al., 2000; Lang and Baker, 2001; Baker, 2002; Groves and Bierlein, 2007). Based on this reasoning, we classify the Naozhi deposit as an intrusion-related gold deposit, an entirely new model for this style of mineralization in the study area.

3.3. The Jiusangou epithermal (HS) gold deposit

Epithermal gold deposits are the most important type of gold deposit in NE China, and occur in a number of different tectonic units. Epithermal deposits discovered in the Yanbian area and adjacent regions include the sub-types, HS and LS. However, some researchers

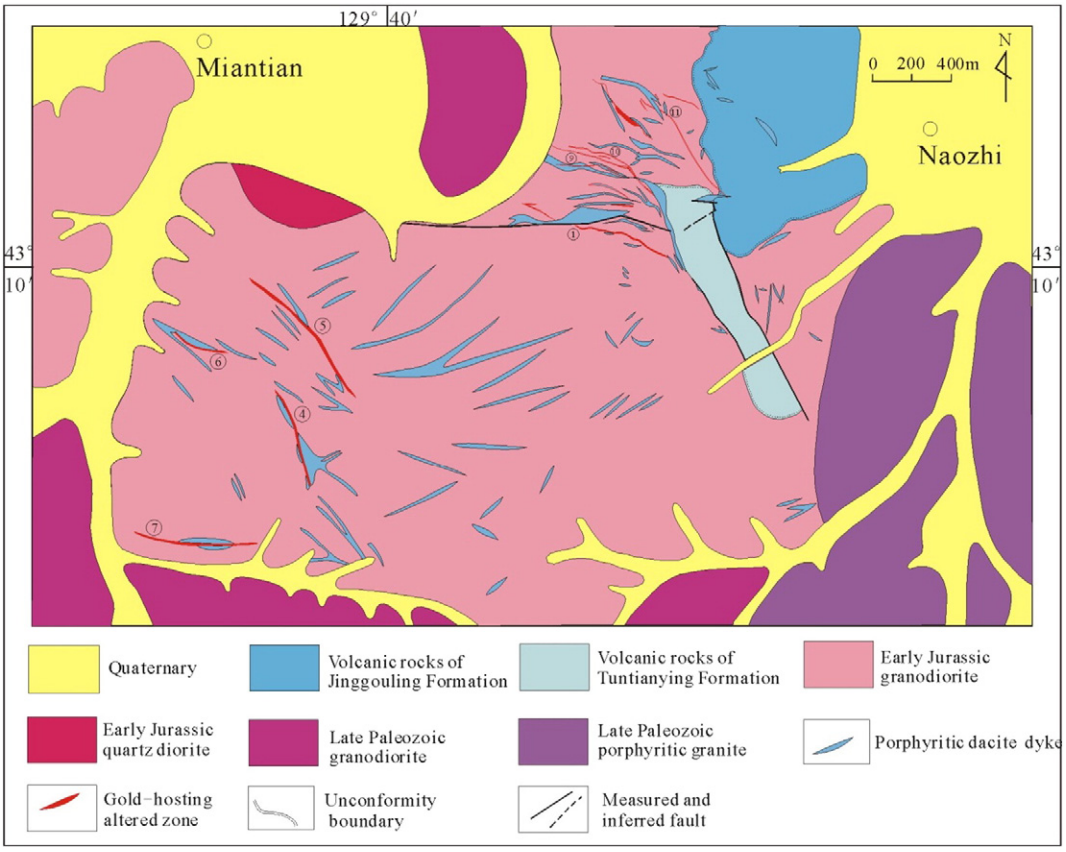

Fig. 3. Geology and gold ore vein distribution sketch map of Naozhi gold deposit.

have suggested that the Jiusangou deposit may not be epithermal but instead may be a magmato-hydrothermal (Zhao et al., 2008) or hypo-mesothermal (Chai et al., 2012) type of deposit, although other research suggests that the Jiusangou deposit is a typical HS subtype epithermal gold deposit (Guan et al., 2010; Han et al., 2013).

The Jiusangou gold deposit is located within the eastern margin of the Duhuangling–Wangqing volcanic basin in the northeastern Yanbian area. This area is dominated by the Late Jurassic continental pyroclastic rocks and lavas (J_3j), and Late Jurassic fine-grained diorite, porphyritic diorite, porphyritic quartz diorite, and porphyritic granite intrusions (Fig. 4). The locations of dike intrusions, alteration zones, and ore-bearing breccia pipes are also controlled by NE–SW, NW–SW, and E–W trending faults.

The mineralization in this area is disseminated or is hosted by vein–stockwork or coarse breccia structures. The ore minerals are generally euhedral and granular, hypidiomorphic and granular, xenomorphic and granular, have relict metasomatic textures, or are cataclastic. The metal minerals in this deposit include pyrite, sphalerite, arsenopyrite, and minor amounts of chalcopyrite; the nonmetal minerals include quartz, sericite, illite, hydromica, epidote, and calcite. Gold is present as native gold and electrum, and is commonly present in intergranular spaces within or as rims around sulfides and quartz.

These data indicate that the Jiusangou deposit is a HS subtype epithermal gold deposit. This inference is supported by the fact that the deposit is hosted by continental volcanic rocks and contains mineralization that is dominantly within breccia pipes. The majority of mineralization within the deposit is hosted by calc-alkaline andesitic and minor high-K calc-alkaline volcanic rocks, and formed at temperatures (250 °C–360 °C) and depths (0.54–2.76 km) that are similar to the majority of typical HS epithermal gold deposits (Chai et al., 2012). This genetic model is also supported by the fact that the mineralization formed from oxidized fluids.

4. Zircon U–Pb dating of intrusions associated with the gold deposits

The formation ages of gold deposits and associated magmatic events were determined by zircon laser ablation-inductively coupled plasma-mass spectrometry (LA-ICP-MS) U–Pb dating of samples from intrusions that are closely associated with gold mineralization in the Wudaogou, Naozhi, and Jiusangou gold deposits.

4.1. Sample locations and descriptions

The granodiorite (sample 13YJG-7) that forms the wall-rocks of the Wudaogou gold deposit has a hypidiomorphic granular texture, is massive, and contains quartz (25%), plagioclase (65%), and amphibole (5%–10%), with minor biotite (Fig. 2). The sample analyzed during this study has undergone silicification and hydrothermal quartz shows equilibrium textures. This silicification is also associated with the alteration of the majority of the plagioclase in this sample to sericite and the alteration of biotite to chlorite and epidote.

Sample YB022-7 from the Naozhi gold deposit is an altered porphyritic dacite dike that was collected from the hanging wall of the main gold-bearing vein within the deposit. This sample is gray–black, porphyritic, massive, and has an interlocking texture, and contains microcrystalline feldspar, felsic minerals and volcanic glass, as well as ~10% quartz and phenocrysts of plagioclase and minor biotite and alkali feldspar. This porphyritic dacite has undergone silicification, and sericite and epidote alteration.

Sample JS2 is from an ore-hosting breccia pipe within the open pit of the Jiusangou gold deposit (Fig. 4). This sample is a massive and porphyritic quartz diorite that contains 30%–40% phenocrysts of mainly plagioclase in a plagioclase, quartz, sericite and minor epidote (<5%) matrix. This intrusion has undergone weak sericite, epidote, and carbonate alteration and has been silicified.

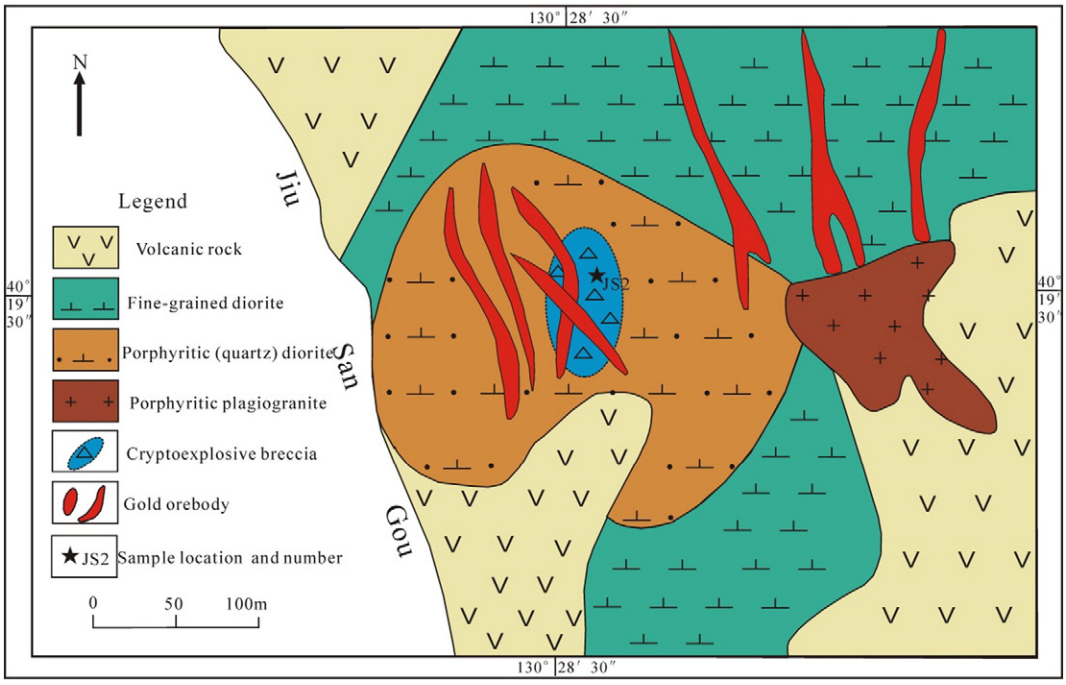

Fig. 4. Geology and orebody distribution map of the Jiusangou gold deposit (modified from Zhao et al., 2008).

4.2. Analytical method

The U–Pb dating of zircons was conducted using a LA-ICP-MS at the State Key Laboratory of Geological Processes and Mineral Resources (GPMR), China University of Geosciences (Wuhan). Laser sampling was performed using a GeoLas 2005. An Agilent 7500a ICP-MS instrument was used to acquire ion-signal intensities. Helium was applied as a carrier gas. Argon was used as the make-up gas and mixed with the carrier gas via a T-connector before entering the ICP. Nitrogen was added into the central gas flow (Ar + He) of the Ar plasma to decrease the detection limit and improve precision (Hu et al., 2008). Each analysis incorporated a background acquisition of approximately 20–30 s (gas blank) followed by 50 s data acquisition from the sample. The Agilent Chemstation was utilized for the acquisition of each individual analysis. Off-line selection and integration of background and analyte signals, and time-drift correction and quantitative calibration for trace element analyses and U–Pb dating were performed by ICPMSDataCal (Liu et al., 2010).

4.3. Results of U–Pb dating of zircon

Cathodoluminescence (CL) images of zircons from different samples are shown in Fig. 5, LA-ICP-MS dating results are listed in Table 2, and U–Pb concordant age diagrams and weighted mean ages are shown in Fig. 6.

Zircons within the Wudaogou granodiorite are euhedral, 50–150 μm in size, and contain magmatic oscillatory zoning (Fig. 5A). The 23 zircons from this sample that were analyzed yielded Th/U ratios of 0.32–0.70, indicating a magmatic origin. Twenty two of these analyses yielded $^{206}Pb/^{238}U$ ages of 262–244 Ma and a weighted mean age of 253.1 ± 0.3 Ma (Fig. 6A), indicating that the granodiorite intrusion was emplaced during the late Permian.

Two zircons from the porphyritic dacite associated with the Naozhi deposit yielded ages of 752 and 320 Ma (Table 2). This result, combined with CL imaging of these zircons (Fig. 5B), indicates that they may be inherited from Paleozoic basement units in this area. The other 17 zircons are divided into two distinct groups. Eight zircons have magmatic oscillatory growth zoning, are of variable size, have short columnar to hypidiomorphic and allotriomorphic crystal shapes, and contain Th and U concentrations of 178.49 ppm to 855.97 ppm (mean of 471.12 ppm) and 297.92 ppm to 1215.25 ppm (mean of 784.38 ppm), respectively, yielding Th/U ratios of 0.43–1.11 (mean of 0.64). One group of zircons yielded U–Pb ages of 203–190 Ma, with a weighted mean age of 198.9 ± 3.6 Ma (Fig. 6C). The other group of 10 analyses included 9 zircons with hypidiomorphic and allotriomorphic shapes, magmatic oscillatory growth zoning, and Th and U concentrations of 118.98 ppm to 591.33 ppm (mean of 274.68 ppm) and 156.05 ppm to 448.42 ppm (mean of 252.00 ppm), respectively, yielding Th/U ratios of 0.65–1.36 (mean of 1.03). These zircons yielded isotopic ages of 130–120 Ma with a weighted mean age of 126.3 ± 1.7 Ma (Fig. 6D).

The majority of the zircons from the Jiusangou porphyritic quartz diorite are intact crystals that are generally long, columnar, and lath-shaped with aspect ratios from 1:1 to 3:1 (Fig. 5C), although individual zircons are irregularly shaped. These zircons contain U and Th concentrations of 146.25 ppm to 763.96 ppm (mean of 289.58 ppm) and 89.60 ppm to 634.76 ppm (mean of 179.20 ppm), respectively, yielding Th/U ratios of 0.45–0.85 that are indicative of a magmatic origin. The 25 analyses of these zircons yielded $^{206}Pb/^{238}U$ ages from 119.3 ± 1.0 to 97.6 ± 0.6 Ma; 18 of these analyses are concordant or plot close to the concordia, yielding $^{206}Pb/^{238}U$ ages from 113.2 ± 0.9 to 104.0 ± 1.0 Ma and a weighted mean age of 108.1 ± 1.4 Ma (mean square weighted deviation (MSWD) = 9.2) (Fig. 6B), which represents the crystallization age of this mineralization-related porphyritic quartz diorite.

5. Discussion

5.1. Orogenic gold deposits in NE China

The Paleozoic history of the eastern segment of CAOB, including the Yanbian area, was dominated by the evolution of the Paleo-Asian ocean tectonic region between the Siberian and the North China cratons. This involved the amalgamation of microcontinental blocks and related orogenic events. Although some orogenic gold mineralization has been discovered in this area (e.g., the Laozuoshan deposit within the Jiamusi

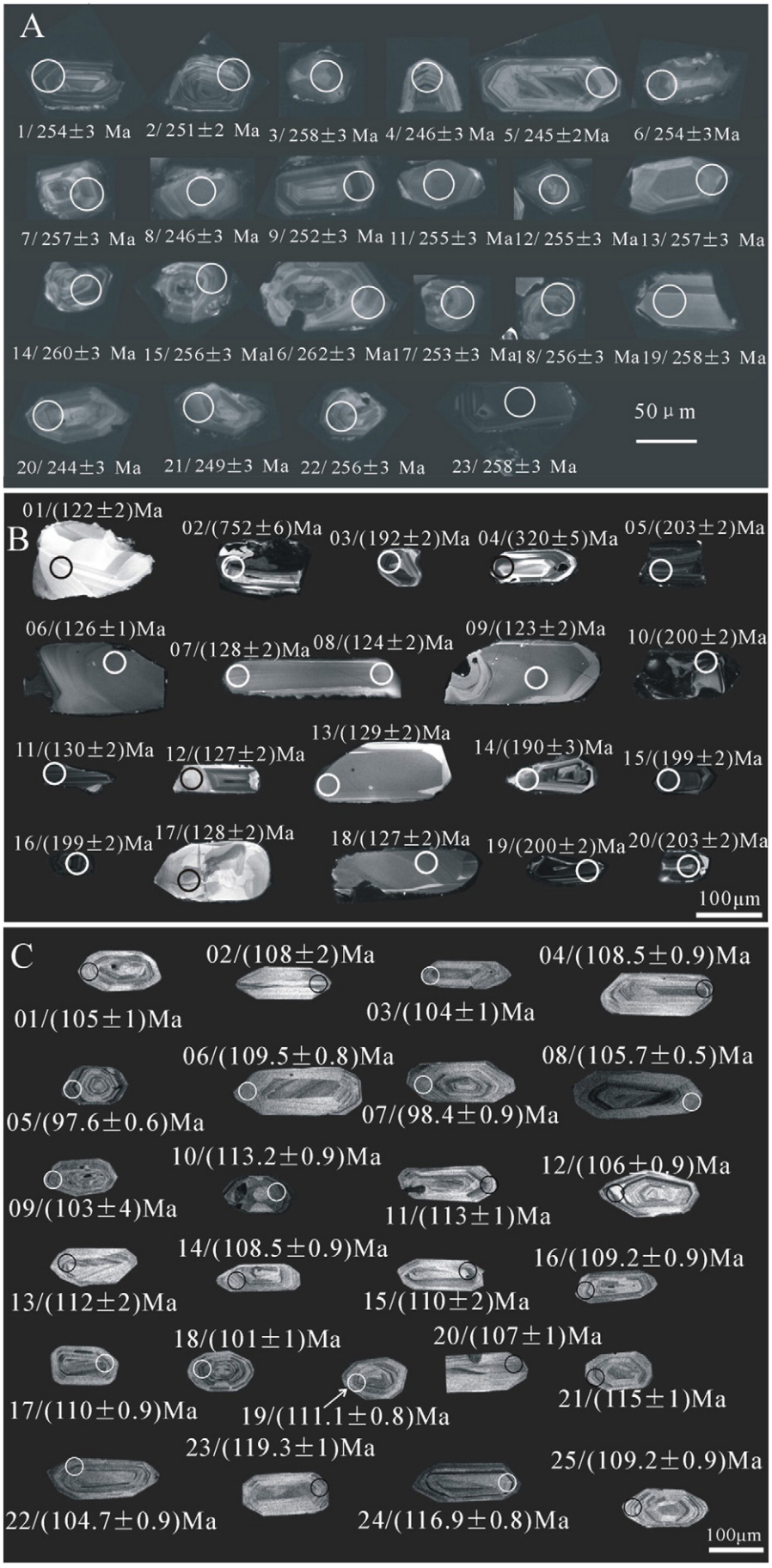

Fig. 5. CL images and dating spots of zircons from the Wudaogou granodiorite (A), Naozhi porphyritic dacite (B) and Jiusangou porphyritic quartz diorite (C).

Table 2
LA-ICP-MS zircon U–Pb data of intrusions in different deposits in Yanbian area.

Analysis point	Composition (10^{-6})		Th/U	U–Th–Pb isotopic ratio						Age (Ma)	
	^{232}Th	^{238}U		$^{207}Pb/^{206}Pb$	1σ	$^{207}Pb/^{235}U$	1σ	$^{206}Pb/^{238}U$	1σ	$^{206}Pb/^{238}U$	1σ
Wudaogou granodiorite (13YJG-7)											
01	678.25	980.39	0.69	0.05206	0.0018	0.2877	0.0098	0.04018	0.00042	254	3
02	734.71	1237.76	0.59	0.05224	0.0014	0.2860	0.0075	0.0397	0.00036	251	2
03	187.00	535.24	0.35	0.05248	0.0023	0.2939	0.0129	0.0409	0.00047	258	3
04	356.93	830.80	0.43	0.05377	0.0018	0.2888	0.0094	0.03892	0.00041	246	3
05	688.53	1159.63	0.59	0.05246	0.0017	0.2797	0.0085	0.03869	0.00035	245	2
06	288.04	693.47	0.42	0.05314	0.0019	0.2936	0.0102	0.04011	0.00043	254	3
07	267.76	638.89	0.42	0.05193	0.002	0.2919	0.0109	0.04067	0.00042	257	3
08	212.98	498.58	0.43	0.0552	0.0026	0.2941	0.0132	0.03895	0.00049	246	3
09	565.17	915.88	0.62	0.05267	0.0018	0.2910	0.0103	0.03991	0.00047	252	3
11	199.10	475.83	0.42	0.05327	0.0022	0.2956	0.0120	0.0404	0.00047	255	3
12	254.99	647.41	0.39	0.05169	0.0019	0.2865	0.0103	0.0403	0.00047	255	3
13	168.65	457.96	0.37	0.05228	0.0022	0.2915	0.0124	0.0406	0.00051	257	3
14	419.32	797.55	0.53	0.05155	0.0017	0.2916	0.0099	0.04114	0.00043	260	3
15	290.43	687.90	0.42	0.05335	0.0021	0.2971	0.0114	0.04058	0.00042	256	3
16	121.09	375.60	0.32	0.05152	0.0024	0.2922	0.0142	0.0415	0.00056	262	3
17	232.91	572.87	0.41	0.05315	0.0023	0.2924	0.0125	0.04006	0.00047	253	3
18	372.59	831.71	0.45	0.05272	0.002	0.2943	0.0111	0.04058	0.00045	256	3
19	278.58	607.16	0.46	0.05281	0.0021	0.2944	0.011	0.04091	0.00049	258	3
20	390.55	798.39	0.49	0.05763	0.0023	0.3021	0.0120	0.03851	0.00046	244	3
21	214.41	533.16	0.40	0.05287	0.0023	0.2836	0.0123	0.03932	0.00046	249	3
22	284.24	648.70	0.44	0.05202	0.0018	0.2906	0.0103	0.04049	0.00046	256	3
23	864.63	1240.49	0.70	0.05159	0.0015	0.2909	0.0087	0.04087	0.0004	258	3
Naozhi porphyritic dacite (YB022-7)											
01	118.98	181.84	0.65	0.1265	0.0072	0.0191	0.0003	0.0066	0.0003	122	2
02	178.49	297.92	0.60	1.1292	0.0380	0.1237	0.0011	0.0378	0.0003	752	6
03	328.33	684.77	0.48	0.2007	0.0094	0.0302	0.0004	0.0093	0.0003	192	2
04	410.04	371.00	1.11	0.4445	0.0163	0.0510	0.0008	0.0157	0.0004	320	5
05	625.86	1301.75	0.48	0.2322	0.0055	0.0319	0.0003	0.0098	0.0002	203	2
06	591.33	448.42	1.32	0.1499	0.0058	0.0197	0.0002	0.0064	0.0001	126	1
07	169.14	156.05	1.08	0.1364	0.0093	0.0200	0.0003	0.0075	0.0002	128	2
08	234.79	219.65	1.07	0.1332	0.0112	0.0194	0.0003	0.0061	0.0001	124	2
09	207.47	225.76	0.92	0.1430	0.0075	0.0192	0.0003	0.0058	0.0002	123	2
10	855.97	1078.89	0.79	0.2208	0.0068	0.0315	0.0003	0.0095	0.0002	200	2
11	524.61	384.83	1.36	0.1664	0.0079	0.0203	0.0003	0.0065	0.0001	130	2
12	255.37	237.84	1.07	0.1417	0.0137	0.0199	0.0003	0.0063	0.0001	127	2
13	224.29	208.92	1.07	0.1365	0.0076	0.0202	0.0003	0.0063	0.0002	129	2
14	495.39	744.42	0.67	0.2292	0.0100	0.0300	0.0005	0.0088	0.0003	190	3
15	337.74	530.67	0.64	0.2261	0.0122	0.0314	0.0003	0.0099	0.0001	199	2
16	523.51	1215.25	0.43	0.2345	0.0092	0.0313	0.0003	0.0098	0.0001	199	2
17	122.46	170.30	0.72	0.1745	0.0092	0.0201	0.0003	0.0080	0.0003	128	2
18	298.33	286.43	1.04	0.1434	0.0065	0.0199	0.0003	0.0065	0.0002	127	2
19	642.47	1099.48	0.58	0.2394	0.0098	0.0315	0.0003	0.0098	0.0001	200	2
20	313.38	519.61	0.60	0.2343	0.0073	0.0319	0.0003	0.0101	0.0002	203	2
Jiusangou porphyritic quartz diorite (JS2)											
01	135.36	242.80	0.56	0.0467	0.0039	0.1063	0.0088	0.0165	0.0002	105	1
02	100.35	146.25	0.69	0.0461	0.0068	0.1073	0.0157	0.0169	0.0003	108	2
03	146.31	228.80	0.64	0.0461	0.0029	0.1033	0.0063	0.0163	0.0002	104	1
04	264.84	361.17	0.73	0.0481	0.0029	0.1125	0.0066	0.0170	0.0001	109	1
06	92.37	185.39	0.50	0.0514	0.0028	0.1213	0.0066	0.0171	0.0001	110	1
08	435.44	701.55	0.62	0.0502	0.0016	0.1145	0.0035	0.0165	0.0001	106	1
10	191.38	327.24	0.58	0.0506	0.0014	0.1229	0.0034	0.0177	0.0001	113	1
11	153.46	256.50	0.60	0.0498	0.0033	0.1212	0.0079	0.0176	0.0002	113	1
12	172.99	342.67	0.50	0.0501	0.0018	0.1145	0.0039	0.0166	0.0001	106	1
13	102.38	185.76	0.55	0.0461	0.0058	0.1109	0.0138	0.0175	0.0003	112	2
14	98.52	195.05	0.51	0.0475	0.0039	0.1111	0.0090	0.0170	0.0002	109	1
15	177.41	211.24	0.84	0.0497	0.0050	0.1177	0.0116	0.0172	0.0003	110	2
16	165.53	303.27	0.55	0.0461	0.0018	0.1085	0.0041	0.0171	0.0001	109	1
17	147.84	276.66	0.53	0.0530	0.0014	0.1252	0.0034	0.0172	0.0001	110	1
19	152.59	268.94	0.57	0.0491	0.0018	0.1175	0.0043	0.0174	0.0001	111	1
20	142.17	166.88	0.85	0.0521	0.0046	0.1204	0.0105	0.0168	0.0002	107	1
22	145.70	252.09	0.58	0.0487	0.0023	0.1099	0.0050	0.0164	0.0002	105	1
25	89.60	193.03	0.46	0.0528	0.0029	0.1245	0.0067	0.0171	0.0001	109	1

massif and the Yangjingou deposit within the Yanbian block), little research has been undertaken on this type of mineralization in NE China.

Zhang (2008) and Wei (2013) suggested that the early stage of formation of the Laozuoshan gold deposit, the second largest gold deposit in Heilongjiang Province, involved orogenic-gold-type mineralization. This deposit is located in the middle part of the Jiamusi massif, an area that records the late Paleozoic collision and amalgamation of the Songliao and Jiamusi blocks. This tectonism caused the formation of deep faults within the collage belt and adjacent areas, all of which induced uplifting of mantle material and the genesis and intrusion of magmas. Simultaneous collision and compression of various blocks also caused intensive ductile and ductile–brittle shearing in this area. The Proterozoic Xingdong Group that hosts the mineralization in this area consists of amphibolite-facies metamorphic rocks that include

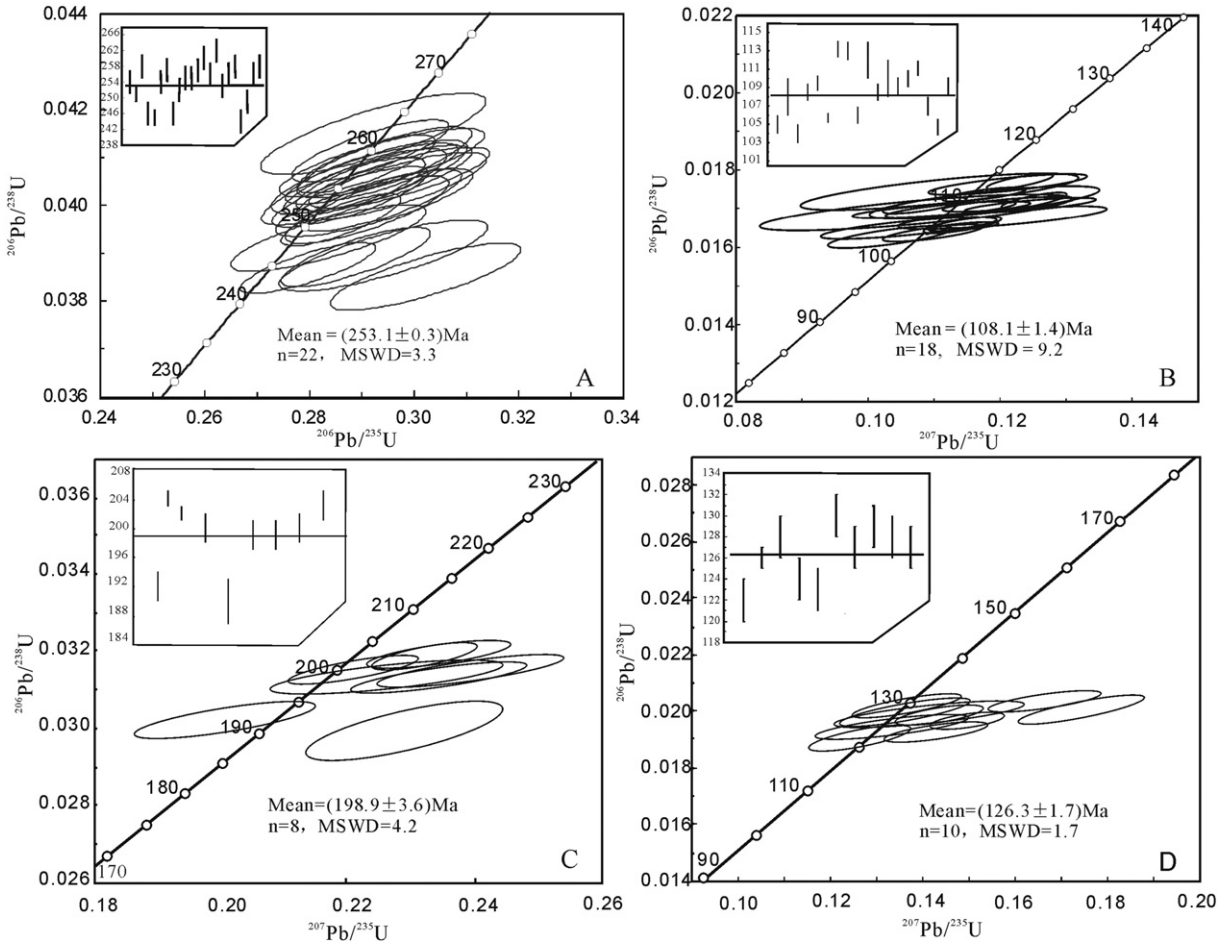

Fig. 6. Concordant diagrams showing U–Pb data and mean age of zircons from the Wudaogou granodiorite (A), Jiusangou porphyritic quartz diorite (B) and Naozhi porphyritic dacite (C, D).

biotite plagiogneiss, graphite schist, marble, banded iron formation (BIF), and garnet–biotite plagiogranulite units. The distribution of these units and the locations of dikes and mineralization are all controlled by NW–SE trending faults. In addition, the gold mineralization in this area is closely related to late Permian and Cretaceous intermediate to acid intrusions, stocks, and dikes, and is present as more than 200 mineralized occurrences within three NW–SW to WNW–ESE trending mineralized zones.

The Laozuoshan gold deposit contains chalcopyrite, arsenopyrite, magnetite, pyrrhotite, chalcocite, sphalerite, native gold, and electrum in a calcite, K-feldspar, quartz, plagioclase, garnet, diopside, and chlorite gangue. The gold mineralization within the deposit is associated with skarn minerals, quartz and sulfide minerals such as pyrite, and arsenopyrite. The geology of the deposit and the ore-forming fluids identified within the system indicate that the deposit underwent two periods of gold mineralization (Wei, 2013). An early phase during the late Permian formed skarn-related orebodies from high–medium salinity, acidic, and weakly reducing fluids at depths of 8.8–9.6 km, as evidenced by the fluid inclusions trapped within the deposit (Wei, 2013). The second event occurred during the Cretaceous and overprints the existing mineralization; this later mineralization formed at depths of 8.0–8.5 km, as evidenced by fluid inclusion data (Wei, 2013). The change in depth of formation between these two periods of mineralization suggests that the two events occurred in different tectonic settings. This inference, combined with the geological characteristics and the geodynamic history of this area, suggests that the earlier late Permian mineralizing event recorded within the Laozuoshan deposit represents the formation of a mesozonal orogenic gold deposit (Groves et al., 1998).

The small Yangjingou gold deposit is located in the Yanbian area, some 11 km south of the large Xiaoxi'nancha gold deposit and 2 km from the large Yangjingou scheelite–quartz deposit (Fig. 2b). The orebodies within the Yangjingou deposit are gold-bearing quartz veins that are generally hosted by or are located along the contact between a late Paleozoic monzogranite and low-grade metamorphic rocks of the Wudaogou Group. The gold mineralization within the deposit is hosted by quartz veins and altered rocks, and is associated with pyrite, arsenopyrite, molybdenite, and chalcopyrite. This mineralization is also associated with silicification, sericite alteration, and phyllic alteration. The conditions of formation, the geology, and the characteristics of the fluids that formed the Yangjingou gold deposit are typical of orogenic gold deposits in China and elsewhere (Groves et al., 1998, 2000). This strongly suggests that the Yangjingou gold deposit is an orogenic gold deposit, the first of this type of deposit to be discovered in the Yanbian region (Zhao et al., 2013).

These data indicate that the Laozuoshan, Yangjingou, and Wudaogou gold deposits are orogenic-type deposits that are closely related to the collision and amalgamation of various microcontinental blocks. Based on this information, we propose that this area is prospective for orogenic gold mineralization and that it should be the focus of further research and exploration.

5.2. Timing of gold deposit formation

5.2.1. Orogenic gold deposits

The U–Pb isotopic dating of 22 zircons from a granodiorite associated with the Wudaogou gold deposit yielded ages between 262 ± 3 and

244 ± 3 Ma and a weighted mean age of 253.1 ± 0.3 Ma (Table 2, Figs. 5A, and 6A), all of which provide evidence of the emplacement age of the granodiorite intrusion. The Wudaogou and Yangjingou gold deposits occur in the same geological setting and formed as a result of the same processes and under the same conditions, indicating that they formed at the same time. This was confirmed by Zhao et al. (2013), who reported an $^{40}Ar/^{39}Ar$ plateau age of 241.57 ± 1.2 Ma for hydrothermal muscovite within auriferous quartz veins in the Yangjingou deposit, an age that is similar to the age of the Wudaogou granodiorite. These data suggest that both the orogenic gold mineralization and the associated magmatism in the Yanbian area occurred between the late Permian and the Early Triassic.

Zircons from a mineralization-related biotite granite within the Laozuoshan orogenic gold deposit in NE China yielded a SHRIMP U–Pb age of 256 ± 3.1 Ma, and molybdenite from this deposit yielded a Re–Os isochron age of 256 Ma, all of which indicate that the early stage of orogenic gold mineralization recorded within the Laozuoshan deposit also formed during the late Permian (Wei, 2013). Therefore, the synchronous formation of the Laozuoshan, Yangjingou, and Wudaogou gold deposits occurred across different tectonic settings. The orogenic Laozuoshan gold deposit formed under the collision between Songliao and Jiamusi blocks (Wei, 2013), while the Yangjingou and Wudaogou were associated with the amalgamation occurring between the North China Craton and the eastern XMOB.

5.2.2. Intrusion-related gold deposits

More than 100 porphyritic dacite dikes are located in NW–SE, NE–SW, and E–W trending swarms in the area around the Naozhi deposit. The majority of the gold orebodies within the deposit are located within or close to these porphyritic dacite dikes, most commonly in the immediate hanging walls and footwalls to these intrusions. Some of the orebodies within the dikes strike sub-parallel to and have the same dip amount and direction as these dikes (Huang, 1997). Some of the orebodies also cross-cut the porphyritic dacite dikes. The spatial relationship between the gold mineralization and the dikes demonstrates that both were controlled by the same tectonic system and formed during the same magmatic event, although the dikes were intruded slightly earlier than the formation of the hydrothermal orebodies.

Zircons within these dikes yield two groups of U–Pb ages. An older group with a weighted mean age of 198.9 ± 3.6 Ma is within error of the zircon U–Pb age of the Naozhi pluton (196 ± 3 Ma; Wu et al., 2011) and is similar to the age of the Miantian pluton (189 ± 1 Ma; Zhang et al., 2002). Therefore, these zircons might have been inherited from earlier-formed plutons in this area. The weighted mean age of the younger group of zircons is 126.3 ± 1.7 Ma, and this represents the timing of crystallization of the porphyritic dacite. Consequently, this area underwent at least two periods of intermediate–acid magmatism during the Mesozoic; i.e., Early Jurassic magmatism formed the batholith-like Miantian and Naozhi granodioritic plutons, and Early Cretaceous intermediate–acid magmatism formed a large number of porphyritic dacite dikes that were intruded along faults and that cross-cut the earlier Early Jurassic granodioritic plutons. Post-magmatic hydrothermal activity then formed gold mineralization along fractures within both the pluton and dikes.

The porphyritic dacite dikes were intruded slightly before the hydrothermal mineralizing event, indicating that the Naozhi gold deposit formed between 120 and 130 Ma. This age is consistent with the ages determined by Meng et al. (2001) using fast neutron activation and by Han et al. (2013), who obtained $^{40}Ar/^{39}Ar$ ages for hydrothermal sericite.

5.2.3. Gold-rich porphyry deposits

The timing of formation of the Xiaoxi'nancha gold deposit, the largest gold deposit in the Yanbian area, remains controversial (Meng et al., 2001; Sun et al., 2008a, 2008b; Ren et al., 2011). For example, Meng et al. (2001) used $^{40}Ar/^{39}Ar$ isotopic dating to obtain an age of 123.35 ± 0.8 Ma for the deposit, whereas Sun et al. (2008a, 2008b) used zircon SHRIMP U–Pb dating to suggest that the gold and copper mineralization within the deposit formed between 104.6 and 102.1 Ma. Ren et al. (2011) used the relationship between recently discovered molybdenite–quartz veins and major gold ore veins, combined with Re–Os dating of six molybdenite samples that formed during the early stages of mineralization, to suggest the deposit formed between a weighted mean age of 109.9 ± 3.9 Ma and an isochron age of 111.1 ± 3.1 Ma. These isotopic dating has led the original late Paleozoic age for this deposit to be rejected in favor of an Early Cretaceous age.

Zircon multi-collector-laser ablation-inductively coupled plasma-mass spectrometry (LA-MC-ICP-MS) dating of a mineralization-related porphyritic biotite granodiorite associated with the Nongping deposit, another example of a gold-rich porphyry deposit in the Yanbian area, led Ren et al. (2012) to suggest that this deposit formed during a Late Cretaceous magmatic event, with the granodiorite being emplaced at 100.04 ± 0.88 Ma. The results of isotopic dating of the Xiaoxi'nancha and Nongping deposits yielded similar results that are also consistent with the age of the No. 18 orebody within the Jinchang gold deposit in the Dongning area of Heilongjiang Province (Table 3).

5.2.4. Epithermal gold deposits

All of the HS and LS epithermal gold deposits in the Yanbian area and adjacent regions formed near-contemporaneously (Table 3). The zircons from the porphyritic quartz diorite within the ore-hosting breccia pipes in the Jiusangou deposit yielded a weighted mean age of 108.1 ± 1.4 Ma (Table 3 and Fig. 6B). In addition, 24 zircons from a quartz diorite closely related to gold mineralization within the Duhuangling deposit yielded a weighted mean age of 118.9 ± 2.2 Ma, which is consistent with the $^{40}Ar/^{39}Ar$ isochron age of fluid inclusions within sulfide–quartz veins in this deposit (Men, 2011).

Zhao et al. (2010) dated fluid inclusions within calcite–quartz veins using $^{40}Ar/^{39}Ar$ isotopic dating and a laser microprobe, yielding an isochron age of 123 ± 7 Ma. Moreover, zircon SHRIMP U–Pb and $^{40}Ar/^{39}Ar$ dating of a porphyritic rhyolite and sericite separated from adularia-bearing auriferous quartz veins that formed during the main stage of mineralization of the Dong'an gold deposit suggest that the deposit formed at 108–107 Ma (Zhang et al., 2010). This result indicates that the gold deposits in the eastern XMOB area formed towards the end of the Early Cretaceous (115–100 Ma), consistent with the dominantly Late Jurassic and Early Cretaceous age of the continental volcanic rocks that form the ore-hosting country rocks of the deposit.

Additional geochronological data for gold deposits of various types within the study area are given in Table 3. These data indicate that three stages of gold metallogenesis have occurred in the study area since the late Paleozoic. The oldest (ca. 270–240 Ma) formed orogenic gold deposits near the Xar Moron–Changchun–Yanji Suture Zone between the North China Craton and the XMOB, including the Yangjingou and Wudaogou deposits. The second stage (ca. 130–120 Ma) formed intrusion-related gold deposits associated with the Naozhi and Miantian plutons in the Wangqing area. The final stage of gold mineralization occurred at ca. 115–100 Ma and was associated with the formation of the majority of mineralization in this area, including the genesis of all of the gold-rich porphyry and epithermal gold deposits. These three stages of gold mineralization are similar in timing to three of the six periods of magmatism in this area; i.e., from the late Permian to the Early Triassic (270–245 Ma), during the early Early Cretaceous (135–120 Ma), and during the late Early Cretaceous (115–105 Ma). Furthermore, the latest two of these stages are also consistent with late Mesozoic events in NE China dated at ca. 140–120 and 115–100 Ma (Ouyang et al., 2013).

5.3. Tectonic setting of gold mineralization

The final closure of the Paleo-Asian Ocean along the Xar Moron–Changchun Suture Zone in NE China is thought to have occurred

Table 3
Geochronological data of some gold deposits in the study area.

Deposit type	Deposit	Rock/ore	Mineral	Age (Ma)	Method	References
Orogenic	Yangjingou	Ore-hosting (metallogenic) monzogranite	Zircon	262.3 ± 1.3	LA-ICP-MS	Zhao et al. (2013)
		Auriferous quartz vein	Hydrothermal muscovite	241.57 ± 1.2	Ar–Ar	Zhao et al. (2013)
	Wudaogou	Ore-hosting (metallogenic) granodiorite	Zircon	253.1 ± 0.3	LA-ICP-MS	This paper
Intrusion-related	Naozhi	Porphyritic dacite vein synchronous with mineralization	Zircon	126.3 ± 1.7	LA-ICP-MS	This paper
		Gold-bearing sulfide–quartz vein	Quartz	123.6 ± 2.5	Ar–Ar	Meng et al. (2001)
Gold-rich porphyry	Xiaoxi'nancha	Altered fine-grained diorite	Zircon	123.45 ± 2.2	SHRIMP	Zhao (2007)
		Post-mineralization porphyritic andesite	Zircon	102.1 ± 2.2	SHRIMP	Zhao (2007)
		Molybdenite–quartz vein	Molybdenite	111.1 ± 3.1	Re–Os isochron	Ren et al. (2011)
	Nongping	Ore-hosting (metallogenic) porphyritic biotite granodiorite	Zircon	100.04 ± 0.88	LA-ICP-MS	Ren et al. (2012)
	No. 18 orebody in Jinchang	Phyllic alteration granite	Sericite	107 ± 5	Rb–Sr isochron	Li et al. (2009)
		Phyllic alteration porphyritic granite dyke	Sericite	110 ± 3	Rb–Sr isochron	Li et al. (2009)
		Porphyritic granite dyke	Zircon	113 ± 2	LA-ICP-MS	Li et al. (2009)
HS epithermal	Jiusangou	Metallogenic porphyritic quartz diorite	Zircon	108.1 ± 1.4	LA-ICP-MS	This paper
		Phyllic alteration porphyritic andesite	Zircon	109.3 ± 2.1	LA-ICP-MS	Men (2011)
	Duhuangling	Metallogenic quartz diorite	Zircon	118.9 ± 2.2	LA-ICP-MS	Men (2011)
		Sulfide–quartz vein	Quartz	107 ± 6	Ar–Ar	Men (2011)
	No. J-1 orebody in Jinchang	Pyrite-bearing quartz vein	Quartz	122.53 ± 0.88	Ar–Ar	Jia et al. (2005)
		Breccias with porphyritic granite cement	Zircon	109.0 ± 2.4	LA-ICP-MS	Han (2010)
LS epithermal	Wufeng–Wuxingshan	Calcite–quartz vein	Quartz	123 ± 7	Ar–Ar	Zhao et al. (2010)

between the late Permian and the Early Triassic, representing the amalgamation of the North China Craton and a group of blocks to the north (the Erguna, Xing'an, Songliao, and Jiamusi blocks; Li, 2006). The A-type granites within the Lesser Hinggan and Zhangguangcai ranges generally formed during the Triassic and the Early Jurassic (Wu et al., 2002; Sun et al., 2004), suggesting that the dominant post-orogenic extensional tectonic regime under the Paleo-Asian ocean weakened during the latest Triassic.

NE China experienced the Late Triassic transformation from a Paleo-Asian Ocean setting to a Circum-Pacific Ocean tectonic regime, a change associated with the emplacement of 220–200 Ma quartz diorite and granodiorite intrusions (Sun et al., 2001, 2005). The Early to Middle Jurassic subduction of the Paleo-Pacific Plate beneath the XMOB resulted in the emplacement of immense volumes of quartz diorite, granodiorite, and monzogranite magmas, as the Early Cretaceous (~145 to 110 Ma) subduction of the Paleo-Pacific Plate caused bimodal volcanism (Sun et al., 2001).

The Yanbian area records the collision between the Jiamusi and Songliao blocks at the end of the early Paleozoic, the collision between the Jiamusi and Khanka blocks during the middle Permian (Xu et al., 2012), and the late Permian to Early Triassic collision between the North China Craton and a group of blocks to the north (the Erguna, Xing'an, Songliao, and Jiamusi blocks) within the XMOB (Sun et al., 2004; Miao et al., 2005; Wu et al., 2011; Zhou et al., 2012). Both the Wudaogou granodiorite and the Yangjingou monzogranite are closely spatially, temporally, and genetically related to orogenic gold mineralization in this area and were emplaced during the Late Permian. These plutons and the gold mineralization are closely related to the collision (and associated orogenesis) between the XMOB and the North China Craton that marked the end of the Paleo-Asian Ocean tectonic regime. The Laozuoshan orogenic gold deposit was considered to form under the late Paleozoic collision and amalgamation of the Songliao and Jiamusi blocks (Wei, 2013).

Late Mesozoic Circum-Pacific tectonism caused the formation of numerous Early Cretaceous gold deposits throughout eastern Asia (Goldfarb et al., 2014), including the largest gold metallogenic belts in Far East Russia (Goryachev and Pirajno, 2014). Ouyang et al. (2013) identified five distinct stages of Mesozoic mineralization and reported that significant continental extension occurred in NE China and surrounding regions between 155 and 120 Ma. This widespread extension ceased during the late Early Cretaceous (115–100 Ma) following rapid changes in tectonic regime during reconfiguration of the Paleo-Pacific Plate.

Goldfarb et al. (2014) suggested that the late Early Cretaceous extension along the Pacific margin caused the formation of epithermal gold deposits in the Okhotsk–Chukotka volcanic belt along the eastern Russia margin, in NE China, and in the SE China fold belt. The Yanbian area was in a continental margin setting between ca. 135 and 120 Ma, associated with oblique subduction of the Paleo-Pacific Plate beneath the Eurasian continent (Pei et al., 2011). This tectonism thinned the lithosphere in this area, leading to the development of a uniform Early Cretaceous volcano-sedimentary basin across all of NE China. This generated intermediate–acid magmas that formed the Tuntianying and Jingouling formations as well as intrusion-related gold mineralization along fractures within early-formed plutons (e.g., the Naozhi and Miantian deposits).

Some porphyry intrusions were emplaced in the eastern Yanbian and Dongning areas during the late Early Cretaceous (ca. 115–100 Ma), generating gold-rich porphyry mineralization (e.g., the Xiaoxi'nancha and Nongping deposits and the No. 18 orebody within the Jinchang deposits) and HS epithermal gold mineralization in volcanic rocks, and cryptoexplosive breccia pipe-hosted mineralization near porphyry intrusions (e.g., the Jiusangou and Duhuangling deposits and the No. J-1 orebody within the Jinchang deposit). Volcanic rocks located far from these intrusions also host LS epithermal gold deposits (e.g., the Ciweigou and Wufeng–Wuxingshan deposits), suggesting that the late Early Cretaceous gold deposits in the study area formed in the same geodynamic setting as the other deposits but formed from fluids with different sources and are hosted by different units.

6. Conclusions

(1) The gold deposits within the Yanbian area and adjacent regions are classified into four types: orogenic, intrusion-related, gold-rich porphyry, and HS and LS epithermal deposits. The orogenic gold deposits are located in the Hunchun area and near the Xar Moron–Changchun Suture Zone, whereas the intrusion-related deposits are hosted by plutons in the Wangqing area, and the gold-rich porphyry and epithermal deposits are located in the eastern Yanbian and Dongning areas.
(2) A mineralized granodiorite associated with the Wudaogou orogenic gold deposit yielded a weighted mean age of 253.1 ±

0.3 Ma, and a porphyritic dacite dike that was emplaced at the time of gold mineralization within the Naozhi intrusion-related gold deposit formed at ca. 126.3 ± 1.7 Ma, an age that probably indicates the timing of formation of gold mineralization within this deposit. Finally, zircons from a porphyritic quartz diorite within an ore-hosting breccia in the Jiusangou epithermal gold deposit yielded a weighted mean age of 108.1 ± 1.4 Ma.

(3) These age data, when combined with previously published data, suggest that this area has undergone three distinct periods of gold metallogenesis, at 270–240, 130–120, and 115–100 Ma. The late Permian to Early Triassic metallogenic event formed orogenic gold deposits such as the Yangjingou and Wudaogou deposits. Intrusion-related gold deposits (e.g., the Naozhi and Miantian deposits) formed during the beginning of the Early Cretaceous, whereas almost all of the gold-rich porphyry and epithermal gold deposits formed during the late Early Cretaceous.

(4) Orogenic gold mineralization in the Yanbian area is closely related to the collision between the North China Craton and the eastern XMOB, an event that was associated with the closure of the Paleo-Asian Ocean. The other types of gold deposit in the study area formed during an Early Cretaceous period of lithospheric extension associated with the post-subduction Paleo-Pacific Plate tectonic regime that influenced this area.

Acknowledgments

This study is supported by the Chinese Ministry of Science and Technology Project (No. 2013CB429802), Science and Technology Development Project of Jilin Province (No. 20120423) and China Geological Survey Project (No. 12120113098300). We would like to thank the Editors of Ore Geology Reviews and Prof. Nie Fengjun, for the invitation to prepare this paper. We also appreciate the assistance from sections and workers in the field work, especially the State Key Laboratory of Geological Processes and Mineral Resources (GPMR), China University of Geosciences (Wuhan) for the zircon U–Pb dating.

References

Baker, T., 2002. Emplacement depth and carbon dioxide-rich fluid inclusions in intrusion-related gold deposits. Econ. Geol. 97, 1111–1117.

Chai, S.L., Zhou, Y.C., Meng, Q.L., 2002. Geological and geochemical characteristics and model of Au (Cu, Ag) deposits associated with volcanic rocks and porphyry in Yanbian Region, Jilin Province. Miner. Depos. 21 (supp.), 94–96 (in Chinese).

Chai, P., Sun, J.G., Men, L.J., Zhang, Y., Han, S.J., Bai, L.A., Liu, Y.S., 2012. U–Pb dating of zircons from host rocks of the Jiusangou gold deposit in Yanbian area and determination of rock-forming and ore-forming epochs. Acta Petrol. Mineral. 9 (5), 634–640 (in Chinese with English abstract).

Cheng, M.H., Xue, X.Y., Li, W.L., 2009. Geologic characteristics of volcanic-type gold deposit in Wangqing County, Naozhi. Jilin Geol. 28 (1), 25–27 (in Chinese with English abstract).

Feng, S.Z., 1998. Metallogenetic and geological features of Wufeng–Wuxingshan gold deposit in Jilin Province. Volcanol. Miner. Resour. 19 (2), 113–118 (in Chinese with English abstract).

Fu, C.L., 2009. The Geochronology, Geochemistry and Petrogenesis of Granitoid from Xiaoxi'nancha in Hunchun Area, Jilin Province. (M.Sc. Thesis), Jilin University, Changchun (in Chinese with English abstract).

Fu, C.L., Sun, D.Y., Wei, H.Y., Gou, J., 2010. Discovery and geologic significance of the Triassic high-Mg diorite in Hunchun area, Jilin Province. Acta Petrol. Sin. 26, 1089–1102 (in Chinese with English abstract).

Goldfarb, R.J., Hart, C., Miller, L., Farmer, G.L., Groves, D.I., 2000. The Tintina gold belt — a global perspective. In: Tucker, T.L., Smith, M.T. (Eds.), The Tintina Gold Belt: Concepts, Exploration and Discoveries. British Columbia and Yukon Chamber of Mines Special vol. 2, pp. 5–34.

Goldfarb, R.J., Groves, D.I., Gardoll, S., 2001. Orogenic gold and geologic time: a global synthesis. Ore Geol. Rev. 18, 1–75.

Goldfarb, R.J., Taylor, R.D., Collins, G.S., Goryachev, N.A., Orlandini, O.F., 2014. Phanerozoic continental growth and gold metallogeny of Asia. Gondwana Res. 25, 48–102.

Goryachev, N.A., Pirajno, F., 2014. Gold deposits and gold metallogeny of Far East Russia. Ore Geol. Rev. 59, 123–151.

Groves, D.I., Bierlein, F.P., 2007. Geodynamic settings of mineral deposit systems. J. Geol. Soc. 164, 19–30.

Groves, D.I., Goldfarb, R.J., Gebre-Mariam, H., Hagemann, S.G., Robert, F., 1998. Orogenic gold deposits: a proposed classification in the context of their crustal distribution and relationship to other gold deposit type. Ore Geol. Rev. 13, 7–27.

Groves, D.I., Goldfarb, R.J., Knox-Robinson, C.M., Ojala, J., Gardoll, S., Yun, G., Holyland, P., 2000. Late-kinematic timing of orogenic gold deposits and significance for computer-based exploration techniques with emphasis on the Yilgarn block, Western Australia. Ore Geol. Rev. 17, 1–38.

Guan, J., Sun, F.Y., Liu, M., 2010. Epithermal gold deposit series in eastern Jilin. Miner. Depos. 29 (supp.), 929–930 (in Chinese).

Han, S.J., 2010. Metallogenic Epoch and Its Geodynamic Significance of the Jinchang Gold Deposit, Heilongjiang Province. (M.Sc. Thesis), Jilin University, Changchun (in Chinese with English abstract).

Han, S.J., Sun, J.G., Bai, L.A., Xing, S.W., Chai, P., Zhang, Y., Yang, F., Men, L.J., Li, Y.X., 2013. Geology and ages of porphyry and medium- to high-sulphidation epithermal gold deposits of the continental margin of northeast China. Int. Geol. Rev. 55 (3), 287–310.

Hou, H.N., Ren, Y.S., Wang, C., Wang, H., Ju, N., 2012. Characteristics of fluid inclusions and significance on ore prospecting of the Ciweigou gold deposit in Yanbian area. Glob. Geol. 31 (4), 704–711.

Hu, Z.C., Gao, S., Liu, Y.S., Hu, S.H., Chen, H.H., Yuan, H.L., 2008. Signal enhancement in laser ablation ICP-MS by addition of nitrogen in the central channel gas. J. Anal. At. Spectrom. 23, 1093–1101.

Huang, G.C., 1997. Discussion on genetic relation between the Naozhi gold deposit and the Mesozoic volcanic rock series in Naozhi, Jilin Province. Miner. Resour. Geol. 11 (57), 32–38.

Jia, D.C., Hu, R.Z., Feng, B.Z., Lu, Y., 2001. Gold–copper metallogenic series and metallogenic model of Mesozoic volcanic belt in Yanbian area, Jilin Province. J. Changchun Univ. Sci. Technol. 31 (3), 224–229 (in Chinese with English abstract).

Jia, D.C., Hu, R.Z., Lu, Y., Qiu, X.L., 2004. Collision belt between the Khanka block and the North China block in the Yanbian region, Northeast China. J. Asian Earth Sci. 23, 211–219.

Jia, G.Z., Chen, J.R., Yang, Z.G., Bian, H.Y., Wang, Y.Z., Liang, H.J., Jin, T.H., Li, Z.H., 2005. Geology and genesis of the superlarge Jinchang gold deposit. Acta Geol. Sin. 79, 661–670 (in Chinese with English abstract).

Jia, D.C., Zhang, X., Lu, Y., Li, L.Z., Gao, W., 2011. Wufeng–Wuxingshan Epithermal Gold Deposit in Yanji, Jilin Province. Geologic Publishing House, Beijing, pp. 6–92 (in Chinese).

Lang, J.R., Baker, T., 2001. Intrusion-related gold systems: the present level of understanding. Mineral. Deposita 36, 477–489.

Li, J.Y., 2006. Permian geodynamic setting of Northeast China and adjacent of regions: closure of the Paleo-Asian Ocean and subduction of the Paleo-Pacific Plate. J. Asian Earth Sci. 26, 207–224.

Li, Z.Z., Li, S.R., Zhang, H.F., 2009. Wall rock alteration and metallogenic chronology of Jinchang gold deposit in Dongning County, Heilongjiang Province. Miner. Depos. 28 (1), 83–92 (in Chinese with English abstract).

Lin, W., Faure, M., Nomade, S., Shang, Q.H., Renne, P.R., 2008. Permian–Triassic amalgamation of Asia: insights from Northeast China sutures and their place in the final collision of North China and Siberia. C. R. Geosci. 340, 190–201.

Liu, Y., Gao, S., Hu, Z., Gao, C., Zong, K., Wang, D., 2010. Continental and oceanic crust recycling-induced melt-peridotite interactions in the Trans-North China orogeny: U–Pb dating, Hf isotopes and trace elements in zircons of mantle xenoliths. J. Petrol. 51, 537–571.

Men, L.J., 2011. An Ore-forming Fluid Study on Late Mesozoic Epithermal Au–Cu Deposits in Yanbian–Dongning Area: Implication for the Metallogenic Mechanism. (Ph.D. Thesis), Jilin University, Changchun (in Chinese with English abstract).

Men, L.J., Sun, J.G., Zhang, Z.J., Li, Y.X., Xing, S.W., Cui, P.L., 2011. An isotopic (Sr, Nd and Pb) tracer study on the Xiaoxinancha gold-rich copper deposit in Yanbian, China: implication for the geodynamic model of diagenesis and metallogenesis. Acta Geol. Sin. (Engl. Ed.) 85 (1), 175–188.

Meng, Q.L., Zhou, Y.C., Chai, S.L., 2001. The Porphyry and Hydrothermal Lode Gold and Copper Deposits in Eastern Yanbian Region of China. Jilin Sci. and Techn. Pub. House, Changchun, pp. 44–156 (in Chinese with English abstract).

Miao, L.C., Qiu, Y.M., Fan, W.M., Zhang, F.Q., Zhai, M.G., 2005. Geology, geochronology, and tectonic setting of the Jiapigou gold deposits, southern Jilin Province, China. Ore Geol. Rev. 26, 137–165.

Ouyang, H.G., Mao, J.W., Santosh, M., Zhou, J., Zhou, Z.H., Wu, Y., Hou, L., 2013. Geodynamic setting of Mesozoic magmatism in NE China and surrounding regions: perspectives from spatio-temporal distribution patterns of ore deposits. J. Asian Earth Sci. 78, 222–236.

Pei, F.P., Xu, W.L., Yang, D.B., Yu, Y., Meng, E., Zhao, Q.G., 2011. Petrogenesis of late Mesozoic granitoids in southern Jilin province, northeastern China: geochronological, geochemical, and Sr–Nd–Pb isotopic evidence. Lithos 125, 27–39.

Qi, J.P., Chen, Y.J., Franco, P., 2005. Geological characteristics and tectonic setting of the epithermal deposits in the Northeast China. J. Miner. Petrol. 25 (2), 47–59 (in Chinese with English abstract).

Ren, Y.S., Wang, H., Qu, W.J., Zhao, H.L., Chu, G.C., 2011. Re–Os isotopic dating of molybdenite from Xiaoxinancha copper–gold deposit in the Yanbian area and its geological significance. J. China Univ. Geosci. (Earth Sci.) 36 (4), 721–728 (in Chinese with English abstract).

Ren, Y.S., Ju, N., Zhao, H.L., Wang, H., Hou, K.J., Liu, S., 2012. Geochronology and geochemistry of metallogenetic porphyry bodies from the Nongping Au–Cu deposit in the eastern Yanbian area, NE China: implications for metallogenic environment. Acta Geol. Sin. (Engl. Ed.) 86 (3), 619–629.

Rui, Z.Y., Zhang, H.T., Wang, L.S., Chen, R.Y., 1995. Porphyry-epithermal copper–gold deposits in Yanbian area, Jilin Province. Miner. Depos. 14 (2), 99-114 (in Chinese with English abstract).

Sillitoe, R.H., 1991. Intrusion-related gold deposits. Gold Metallogeny and Exploration, pp. 165–209.
Su, F.X., Wang, X.Y., Jia, W.G., Zhang, C.H., Liang, H.J., 2003. Study on typomorphic characteristics of pyrite in the Naozhi gold deposit, Jilin. Gold 24 (5), 13–16 (in Chinese with English abstract).
Sun, D.Y., Lin, Q., Wu, F.Y., Lu, X.P., 2001. Petrogenesis and crust–mantle interaction of early Yanshanian Baishishan pluton in Zhangguangcai Range. Acta Petrol. Sin. 17 (2), 227–235 (in Chinese with English abstract).
Sun, D.Y., Wu, F.Y., Zhang, Y.B., Gao, S., 2004. The final closing time of the west Lamulun River–Changchun–Yanji plate suture zone — evidence from the Dayushan granitic pluton, Jilin Province. J. Jilin Univ. (Earth Sci. Ed.) 34, 174–181 (in Chinese with English abstract).
Sun, D.Y., Wu, F.Y., Gao, S., Lu, X.P., 2005. Confirmation of two episodes of A-type granite emplacement during Late Triassic and Early Jurassic in the central Jilin Province, and their constraints on the structural pattern of Eastern Jilin–Heilongjiang Area, China. Earth Sci. Front. 12 (2), 263–275 (in Chinese with English abstract).
Sun, J.G., Chen, L., Zhao, J.K., Men, L.J., Pang, W., Chen, D., Liang, S.N., 2008a. SHRIMP U–Pb dating of zircons from Late Yanshanian granitic complex in Xiaoxinancha gold-rich copper orefield of Yanbian and its geological implications. Miner. Depos. 27 (3), 319–328 (in Chinese with English abstract).
Sun, J.G., Men, L.J., Zhao, J.K., Chen, L., Liang, S.N., Chen, D., Pang, W., 2008b. Zircon chronology of melanocratic dykes in the district of the Xiaoxinancha Au-rich Cu deposit in Yanbian and its Geological implication. Acta Geol. Sin. 82 (4), 517–527 (in Chinese with English abstract).
Thompson, J.F.H., Sillitoe, R.H., Baker, T., Lang, J.R., Mortensen, J.K., 1999. Intrusion-related gold deposits associated with tungsten–tin provinces. Mineral. Deposita 34, 323–334.
Wei, L.X., 2013. Study on Metallogenic Regularity and Quantitative Prediction of Nonferrous Metals and Precious Metals in Heilongjiang Province. (Ph.D. Thesis), Jilin University, Changchun (in Chinese with English abstract).
Wu, T.T., 2013. Geological Characteristics and Metallogenic Regularity of Gold Deposits from Naozhi to Duhuangling in Wangqing County, Jilin Province. (M.Sc. Thesis), Jilin University, Changchun (in Chinese with English abstract).
Wu, F.Y., Sun, D.Y., Li, H.M., Jahn, B.M., Wilde, S.A., 2002. A-type granites in northeastern China: age and geochemical constraints on their petrogenesis. Chem. Geol. 187, 143–173.
Wu, F.Y., Zhao, G.C., Sun, D.Y., Wilde, S.A., Zhang, G.L., 2007. The Hulan Group: its role in the evolution of the Central Asian Orogenic Belt of NE China. J. Asian Earth Sci. 30, 542–556.
Wu, F.Y., Sun, D.Y., Ge, W.C., Zhang, Y.B., Grant, M.L., Wilde, S.A., Jahn, B.M., 2011. Geochronology of the Phanerozoic granitoids in northeastern China. J. Asian Earth Sci. 41, 1–30.
Xu, W.L., Wang, F., Meng, E., Gao, F.H., Pei, F.P., Yu, J.J., Tang, J., 2012. Paleozoic–Early Mesozoic tectonic evolution in the eastern Heilongjiang province, NE China: evidence from igneous rock association and U–Pb geochronology of detrital zircons. J. Jilin Univ. (Earth Sci. Ed.) 42 (5), 1378–1389 (in Chinese with English abstract).
Zhang, Y.B., 2002. The Isotopic Geochronologic Frame of Granitic Magmatism in Yanbian Area. (Ph.D. Thesis), Jilin University, Changchun (in Chinese with English abstract).
Zhang, L.Y., 2008. Study on geological characteristics and enrichment regularities of gold mineralization in Laozuoshan gold deposit, Heilongjiang province. (M.Sc. Thesis), Jilin University, Changchun (in Chinese with English abstract).
Zhang, Y.B., Wu, F.Y., Sun, D.Y., Li, H.M., 2002. Single grain zircon U–Pb ages of the "Early Hercynian" Miantian granites and Zhongping hypersthene diorite in the Yanbian area. Geol. Rev. 48 (4), 424–429 (in Chinese with English abstract).
Zhang, Z.C., Mao, J.W., Wang, Y.B., Pirajno, F., Liu, J.L., Zhao, Z.D., 2010. Geochemistry and geochronology of the volcanic rocks associated with the Dong'an adularia–sericite epithermal gold deposit, Lesser Hinggan Range, Heilongjiang province, NE China: constraints on the metallogenesis. Ore Geol. Rev. 37, 158–174.
Zhang, H.D., Zhang, H.F., Santosh, M., Li, S.R., 2014. Fluid inclusions from the Jinchang Cu–Au deposit, Heilongjiang Province, NE China: genetic style and magmatic–hydrothermal evolution. J. Asian Earth Sci. 82, 103–114.
Zhao, H.G., 2007. Study on the Metallogenesis and Models in Mesozoic Epithermal Gold Deposits in Yanbian, Jilin Province. (Ph.D. Thesis), Jilin University, Changchun (in Chinese with English abstract).
Zhao, H., Cui, X.W., Xu, L.X., 2008. Discussion on geology and isotope characters of Jiusangou gold deposit in Wangqing, Jilin Province. Gold Sci. Technol. 16 (1), 48–51 (in Chinese with English abstract).
Zhao, Y.J., Sun, J.G., Wang, Q.H., Men, L.J., Li, Y.X., Guo, J., 2010. $^{40}Ar/^{39}Ar$ laser probe dating and discussion on metallogenic epoch of epithermal Au–Cu deposit in Yanbian area of Jilin. Earth Sci. Front. 17 (2), 156–169 (in Chinese with English abstract).
Zhao, H.L., Ren, Y.S., Hou, H.N., Wang, H., Ju, N., Chen, C., Li, C.H., 2013. Metallogenic age and tectonic setting of the first orogenic gold deposit discovered in the Yanbian region, NE China. Int. Geol. Rev. 55 (7), 882–893.
Zhou, J.B., Zeng, W.S., Cao, J.L., Han, J., Guo, X.D., 2012. The tectonic framework and evolution of the NE China: from ~500 Ma to ~180 Ma. J. Jilin Univ. (Earth Sci. Ed.) 42 (5), 1298–1316 (in Chinese with English abstract).